

## *Supplementary Materials*

# **Spectroscopic and microscopic analyses of Fe<sub>3</sub>O<sub>4</sub>/Au nanoparticles obtained by laser ablation in water**

**Maurizio Muniz-Miranda,<sup>1,2,\*</sup> Francesco Muniz-Miranda,<sup>3</sup> Emilia Giorgetti<sup>2</sup>**

<sup>1</sup> Department of Chemistry "Ugo Schiff", University of Florence, Via Lastruccia 3, 50019 Sesto Fiorentino, Italy; maurizio.muniz@unifi.it

<sup>2</sup> Institute of Complex Systems (CNR), Via Madonna del Piano 10, 50019 Sesto Fiorentino, Italy; emilia.giorgetti@fi.isc.cnr.it

<sup>3</sup> École Nationale Supérieure de Chimie de Paris and PSL Research University, CNRS, Institute of Chemistry for Life and Health Sciences (i-CLeHS), FRE 2027, 11, rue Pierre et Marie Curie, F-75005 Paris, France; f.muniz-miranda@chimieparistech.psl.eu

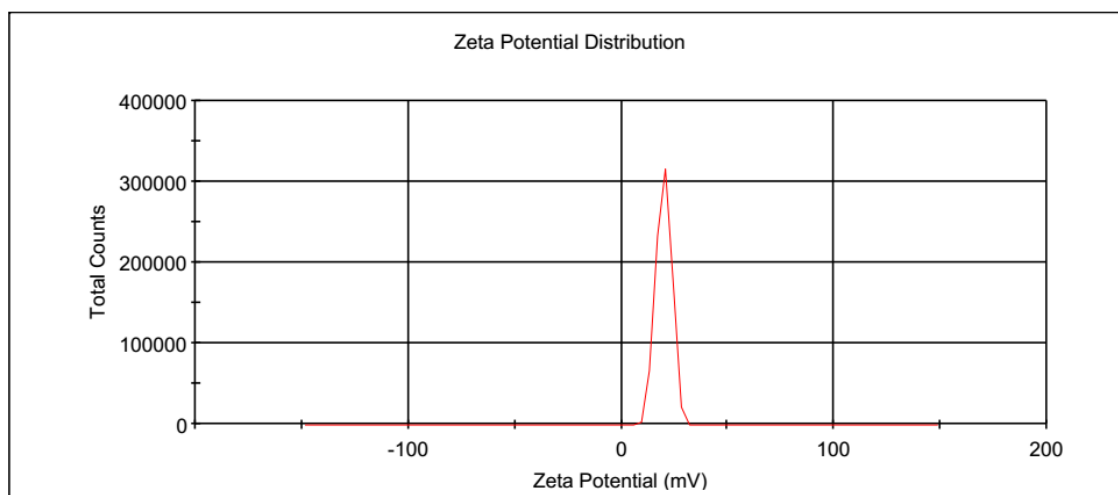
\* Correspondence: maurizio.muniz@unifi.it

Sample Name: Fe\_ns

Results

|                                      | Mean (mV)           | Area (%) | Width (mV) |
|--------------------------------------|---------------------|----------|------------|
| <b>Zeta Potential (mV):</b> 20.0     | <b>Peak 1:</b> 20.0 | 100.0    | 3.63       |
| <b>Zeta Deviation (mV):</b> 3.63     | <b>Peak 2:</b> 0.00 | 0.0      | 0.00       |
| <b>Conductivity (mS/cm):</b> 0.00662 | <b>Peak 3:</b> 0.00 | 0.0      | 0.00       |

Result quality **Good**



Sample Name: Au\_ns .-> Fe\_ns

Results

|                                     | Mean (mV)           | Area (%) | Width (mV) |
|-------------------------------------|---------------------|----------|------------|
| <b>Zeta Potential (mV):</b> 13.9    | <b>Peak 1:</b> 13.9 | 100.0    | 4.17       |
| <b>Zeta Deviation (mV):</b> 4.17    | <b>Peak 2:</b> 0.00 | 0.0      | 0.00       |
| <b>Conductivity (mS/cm):</b> 0.0167 | <b>Peak 3:</b> 0.00 | 0.0      | 0.00       |

Result quality **Good**

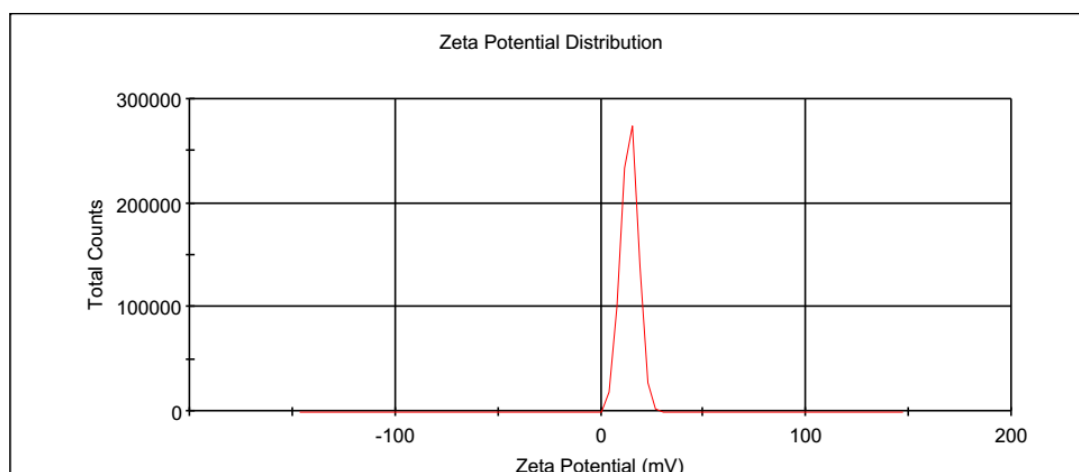
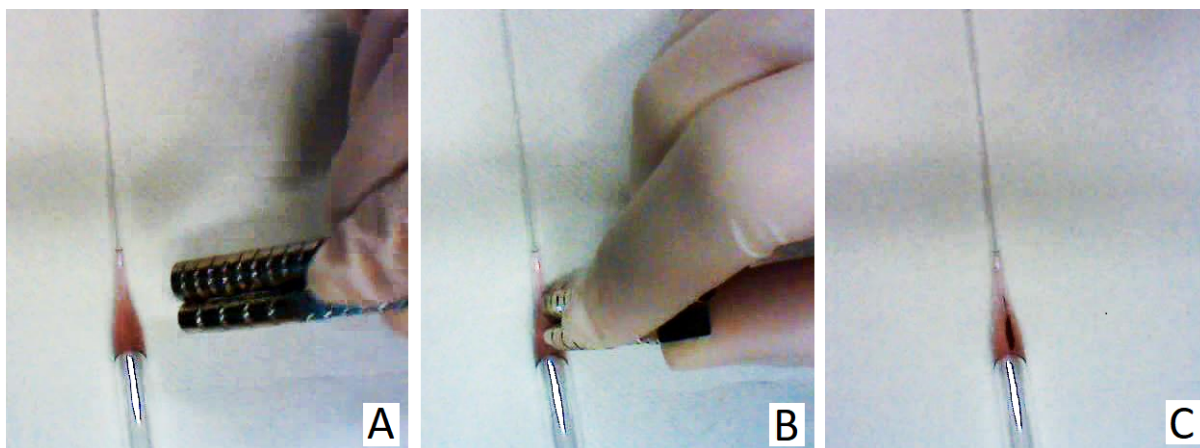
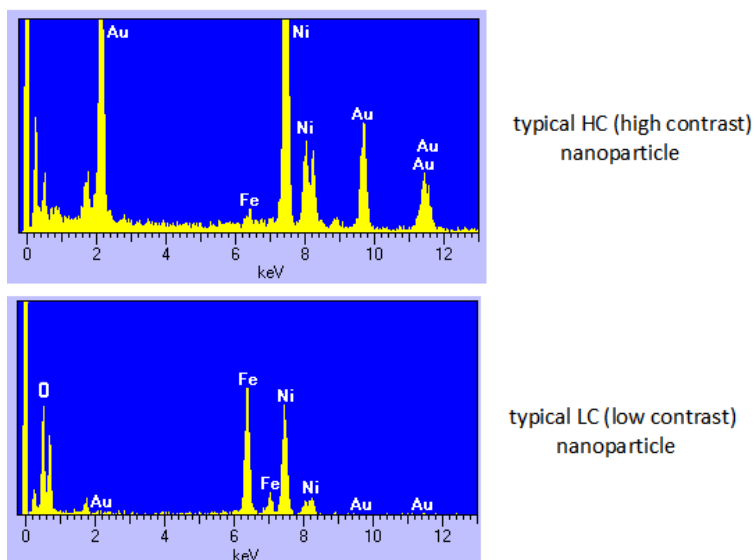


Fig. S1 – Zeta potential values for the colloid obtained by laser ablation of Fe (above) and for that obtained by two-step laser ablation of Fe and then of Au (below).



**Fig. S2 –  $\text{Fe}_3\text{O}_4/\text{Au}$  bimetallic colloidal sample, as obtained by two-step laser ablation (A), after application of magnetic field (B) and after successive removing of the magnet (C).**



**Fig. S3 - EDX analysis of HC and LC nanoparticles.**

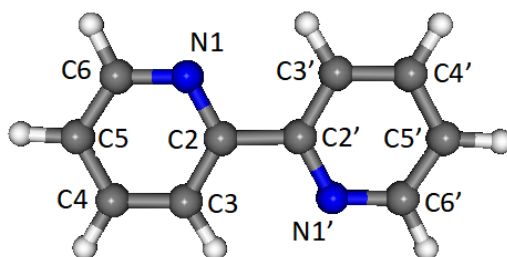


**TABLE S1 – Structural parameters of bpy.**

| Bond distances/Å | Experimental data <sup>a</sup> | B3LYP/6-31G(+*) <sup>b</sup> | B3LYP/LanI2dz <sup>c</sup> |
|------------------|--------------------------------|------------------------------|----------------------------|
| N1C2             | 1.35                           | 1.353                        | 1.339                      |
| C2C3             | 1.41                           | 1.406                        | 1.398                      |
| C3C4             | 1.40                           | 1.395                        | 1.385                      |
| C4C5             | 1.37                           | 1.398                        | 1.389                      |
| C5C6             | 1.37                           | 1.399                        | 1.390                      |
| C6N1             | 1.37                           | 1.343                        | 1.329                      |
| C2C2'            | 1.50                           | 1.490                        | 1.489                      |
|                  |                                |                              |                            |
| Bond angles/°    | Experimental data <sup>a</sup> | B3LYP/6-31G(+*) <sup>b</sup> | B3LYP/LanI2dz <sup>c</sup> |
| N1C2C3           | 122.5                          | 122.3                        | 122.5                      |
| C2C3C4           | 118.3                          | 119.0                        | 118.9                      |
| C3C4C5           | 119.7                          | 118.9                        | 119.1                      |
| C4C5C6           | 118.5                          | 118.1                        | 118.5                      |
| C5C6N1           | 124.3                          | 123.7                        | 123.5                      |
| C6N1C2           | 116.7                          | 117.9                        | 118.5                      |
| N1C2C2'          | 116.1                          | 116.8                        | 117.1                      |
| C3C2C2'          | 121.4                          | 120.9                        | 120.9                      |

<sup>a</sup> : Merritt. L.L. Jr, Schroeder E.D. *Acta Cryst.* **1956**, *9*, 801.

<sup>b</sup> : Ould-Moussa, L.; Castella-Ventura, M.; Kassab, E.; Poizat, O.; Strommen, D.P.; Kincaid, J.R. *J. Raman Spectrosc.* **2000**, *31*, 377–390.

<sup>c</sup> : present work.

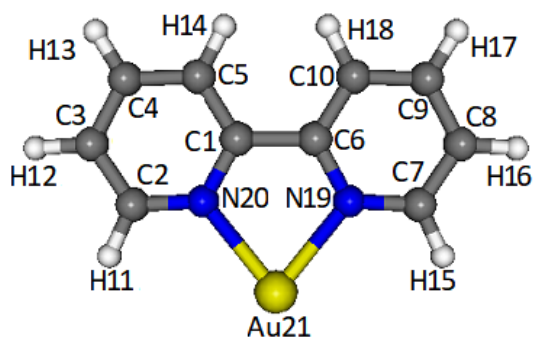
**TABLE S2 – Observed and calculated vibrational frequencies (cm<sup>-1</sup>) of bpy.**

| Symmetry species | IR/Raman <sup>a</sup> | B3LYP/<br>6-31G(+*) <sup>a</sup> | B3LYP/<br>LanI2dz <sup>b</sup> |
|------------------|-----------------------|----------------------------------|--------------------------------|
| A <sub>g</sub>   | 1589                  | 1585                             | 1597                           |
| B <sub>u</sub>   | 1575                  | 1582                             | 1595                           |
| A <sub>g</sub>   | 1572                  | 1567                             | 1582                           |
| B <sub>u</sub>   | 1550                  | 1554                             | 1564                           |
| A <sub>g</sub>   | 1482                  | 1474                             | 1487                           |
| A <sub>g</sub>   | 1446                  | 1445                             | 1443                           |
| B <sub>u</sub>   | 1450                  | 1450                             | 1454                           |
| B <sub>u</sub>   | 1410                  | 1423                             | 1418                           |
| A <sub>g</sub>   | 1309                  | 1309                             | 1326                           |
| A <sub>g</sub>   | 1301                  | 1299                             | 1314                           |
| B <sub>u</sub>   | 1265                  | 1281                             | 1308                           |
| B <sub>u</sub>   | 1250                  | 1254                             | 1270                           |
| A <sub>g</sub>   | 1236                  | 1241                             | 1274                           |
| B <sub>u</sub>   | 1140                  | 1167                             | 1170                           |
| A <sub>g</sub>   | 1146                  | 1166                             | 1170                           |
| B <sub>u</sub>   | 1085                  | 1091                             | 1093                           |
| A <sub>g</sub>   | 1094                  | 1099                             | 1100                           |
| B <sub>u</sub>   | 1065                  | 1066                             | 1070                           |
| A <sub>g</sub>   | 1044                  | 1041                             | 1042                           |
| B <sub>g</sub>   | -----                 | 1009                             | 1038                           |
| B <sub>u</sub>   | 1040                  | 1034                             | 1036                           |
| A <sub>u</sub>   | -----                 | 1008                             | 1033                           |
| B <sub>u</sub>   | 995                   | 982                              | 985                            |
| A <sub>g</sub>   | 994                   | 990                              | 981                            |
| A <sub>u</sub>   | 975                   | 975                              | 973                            |
| B <sub>g</sub>   | -----                 | 972                              | 991                            |
| B <sub>g</sub>   | 909                   | 915                              | 933                            |
| B <sub>u</sub>   | 890                   | 905                              | 930                            |
| B <sub>g</sub>   | 815                   | 830                              | 837                            |
| A <sub>g</sub>   | 764                   | 762                              | 767                            |
| A <sub>u</sub>   | 755                   | 763                              | 782                            |
| B <sub>g</sub>   | 742                   | 740                              | 762                            |
| A <sub>u</sub>   | 740                   | 743                              | 759                            |
| B <sub>u</sub>   | 655                   | 659                              | 660                            |
| B <sub>u</sub>   | 620                   | 629                              | 624                            |
| A <sub>g</sub>   | 614                   | 622                              | 619                            |
| B <sub>g</sub>   | 550                   | 564                              | 566                            |
| A <sub>u</sub>   | -----                 | 439                              | 442                            |
| A <sub>g</sub>   | 440                   | 435                              | 440                            |
| B <sub>g</sub>   | 409                   | 409                              | 419                            |
| A <sub>u</sub>   | 400                   | 402                              | 412                            |
| A <sub>g</sub>   | 332                   | 325                              | 329                            |
| B <sub>g</sub>   | 224                   | 222                              | 227                            |

<sup>a</sup> : Ould-Moussa, L.; Castella-Ventura, M.; Kassab, E.; Poizat, O.; Strommen, D.P.; Kincaid, J.R. *J. Raman Spectrosc.* **2000**, *31*, 377–390.

<sup>b</sup> : present work.

**TABLE S3 – Mulliken partial charges.**



| bpy/Au <sup>+</sup> complex |         | bpy/Au <sup>0</sup> complex |         |
|-----------------------------|---------|-----------------------------|---------|
| C1                          | 0.2674  | C1                          | 0.1428  |
| C2                          | -0.2083 | C2                          | -0.2710 |
| C3                          | -0.1387 | C3                          | -0.1619 |
| C4                          | -0.1678 | C4                          | -0.1900 |
| C5                          | -0.2392 | C5                          | -0.2860 |
| C6                          | 0.2674  | C6                          | 0.1428  |
| C7                          | -0.2083 | C7                          | -0.2710 |
| C8                          | -0.1387 | C8                          | -0.1619 |
| C9                          | -0.1678 | C9                          | -0.1900 |
| C10                         | -0.2392 | C10                         | -0.2860 |
| H11                         | 0.2648  | H11                         | 0.2571  |
| H12                         | 0.2665  | H12                         | 0.2346  |
| H13                         | 0.2707  | H13                         | 0.2380  |
| H14                         | 0.2422  | H14                         | 0.2364  |
| H15                         | 0.2648  | H15                         | 0.2571  |
| H16                         | 0.2665  | H16                         | 0.2346  |
| H17                         | 0.2707  | H17                         | 0.2380  |
| H18                         | 0.2422  | H18                         | 0.2364  |
| N19                         | -0.3064 | N19                         | -0.0840 |
| N20                         | -0.3064 | N20                         | -0.0840 |
| Au21                        | 0.4979  | Au21                        | -0.2323 |

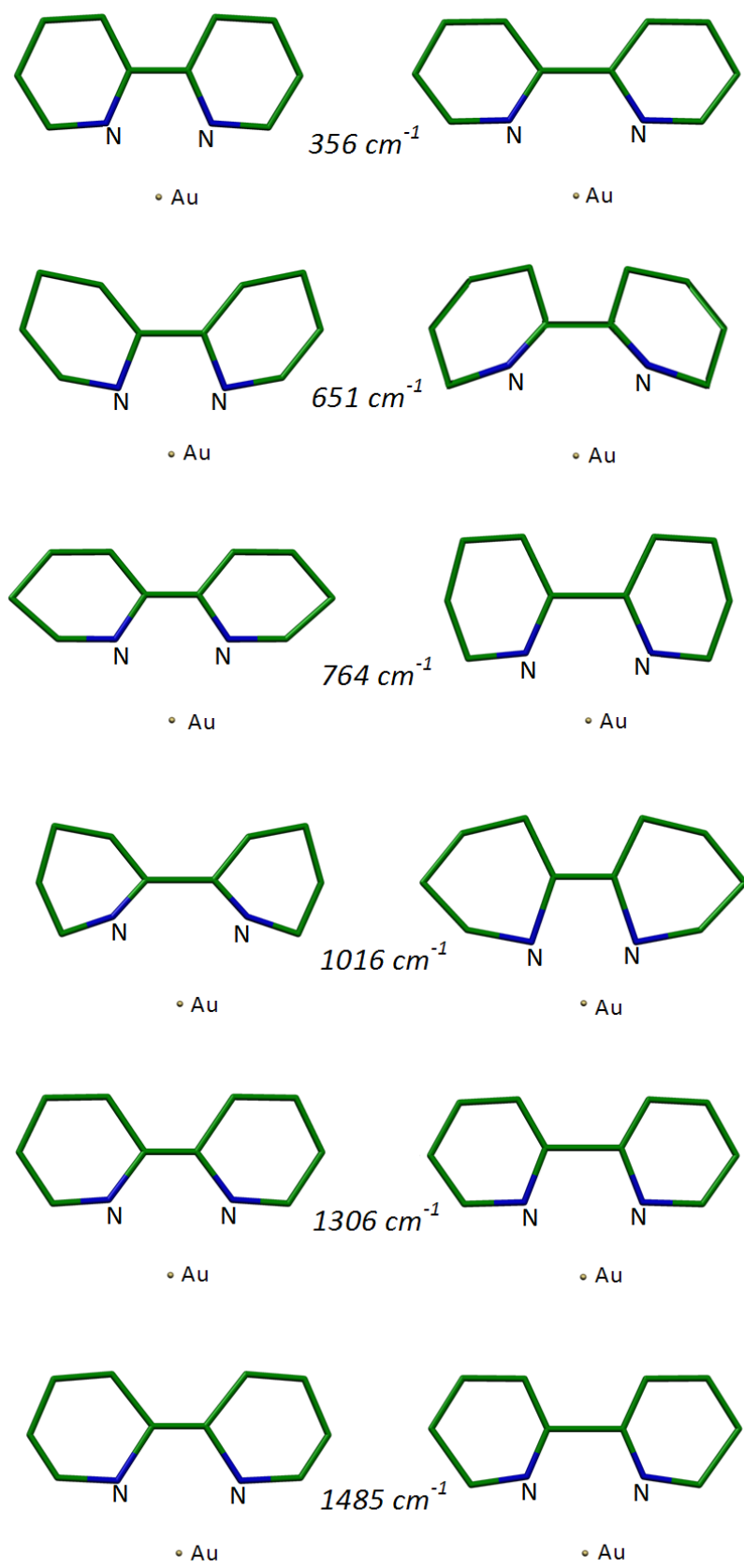


**Fig. S4 – Calculated normal modes of the bpy/Au<sup>+</sup> complex relative to the prominent SERS bands. The hydrogen atoms are omitted.**

## Details on the $D_{CT}$ calculations

The  $D_{CT}$  (charge-transfer distance) index was proposed to define a measure of the length of charge transfer (CT) excitation, as well as the amount of the transferred charge. This is achieved from the total electronic density computed for the ground and excited states, or adopting a suitable partition scheme for atomic charges (like Mulliken's).

However, the  $D_{CT}$  descriptor can be adopted also for ground states of systems with different components, as long as the geometry of common moieties of the relaxed systems do not change significantly.

In the case investigated in this paper, the previous statement is equivalent to say that the full Hamiltonian of the system ( $H_{total}$ , with total=bpy+gold) can be solved on the bases of the Hamiltonians of the subsystems ( $H_{bpy}$  and  $H_{gold}$ ).

In practice, to compute the  $D_{CT}$  here we have followed this procedure:

1. we have obtained the relaxed geometry of the (bpy + Au<sup>+</sup>) system;
2. for the starting state, we have given to bpy atoms the Mulliken charges of the isolated bpy and we have put a zero charge on the gold atom coordinates;
3. for the final state, we have given to the (bpy + Au<sup>+</sup>) system their respective Mulliken charges;
4. finally, we have calculated the  $D_{CT}$  descriptor using the spreadsheet reported in the Supplementary Materials of ref. 56.

.....  
56. Jacquemin, D.; Le Bahers, T.; Adamo, C.; Ciofini, I. What is the "best" atomic charge model to describe through-space charge-transfer excitations? *Phys. Chem. Chem. Phys.* **2012**, *14*, 5383–5388.



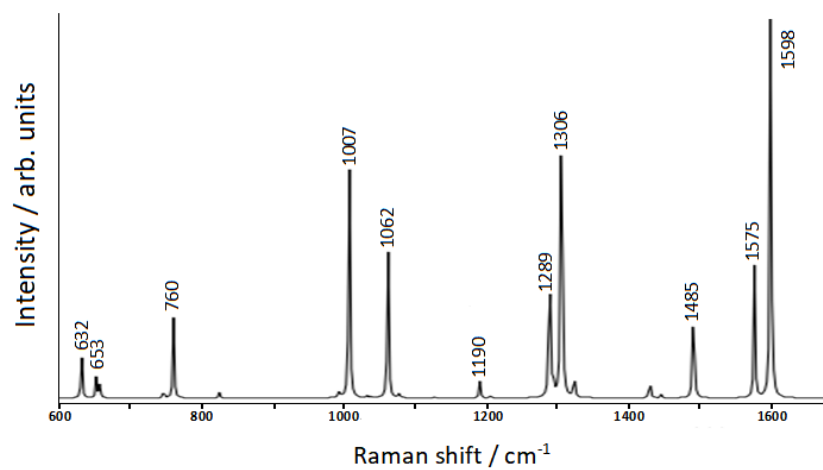


**Fig. S5 – Simulated SERS spectrum for the bpy/Au<sup>+</sup> complex.**